Acta Materialia 165 (2019) 398–408

Contents lists available at ScienceDirect

Acta Materialia

journal homepage: www.elsevier.com/locate/actamat

Full length article

The role of point defects and defect gradients in flash sintering of perovskite oxides

Wolfgang Rheinheimer [a, b, *], Xin Li Phuah [a], Han Wang [a], Fabian Lemke [c], Michael J. Hoffmann [b], Haiyan Wang [a, d]

[a] School of Materials Engineering, Purdue University, West Lafayette, IN, 47907, USA
[b] Institute of Applied Materials – Ceramic Materials and Technologies (IAM-KWT), Karlsruhe Institute of Technology (KIT), 76131, Karlsruhe, Germany
[c] Robert Bosch GmbH, Department of Corporate Research, Stuttgart, Germany
[d] School of Electrical and Computer Engineering, Purdue University, West Lafayette, IN, 47907, USA

ARTICLE INFO

Article history:
Received 18 September 2018
Received in revised form
6 December 2018
Accepted 6 December 2018
Available online 7 December 2018

Keywords:
Flash sintering
Space charge
Strontium titanate
Point defects
Non-stoichiometry

ABSTRACT

The present study investigates the impact of point defects and their redistribution on the flash sintering process. Strontium titanate was chosen as a model system for the group of perovskite ceramics. The characteristics of flash sintering of strontium titanate were analyzed with different acceptor dopant concentrations. The onset of flash sintering was found to be dependent on the acceptor dopant concentration, as expected by the increasing conductivity. A gradient in the microstructure was found after flash sintering with larger grain sizes at the negative electrode. TEM-EDS measurements indicated Ti enrichment at the positive electrode for undoped strontium titanate and strong acceptor segregation for doped strontium titanate. In contrast, grain boundaries at the negative electrode were found to be stoichiometric for the undoped case and the acceptor segregation was less obvious for the doped case.

Based on these results and the space charge behavior of strontium titanate, we infer that a gradient of the oxygen vacancy concentration is induced by the electric field during flash sintering: at the positive electrode the oxygen vacancy concentration is higher than at the negative electrode. For strontium titanate it is well known that a high oxygen vacancy concentration reduces the space charge and, hence, acceptor segregation, which agrees well with the experimental findings. Overall, the present study highlights the importance of point defect gradients and space charge for flash sintering of strontium titanate, which may be applicable for many other functional ceramics.

Published by Elsevier Ltd on behalf of Acta Materialia Inc.

1. Introduction

Flash sintering is a new field-assisted sintering process which was first demonstrated in 2010 [1]. This novel sintering technique involves electric currents to induce self-heating of a ceramic material. For this process, a voltage is applied to a green body which is preheated in a conventional furnace. Since the conductivity of most ceramics increases with temperature, there will be an increase of current flowing through the green body during the heating process. If the conductivity has increased enough to allow a significant current, Joule heating occurs in the green body, yielding a temperature increase over the furnace temperature. Eventually, a thermal runaway occurs resulting in an abrupt increase in current and sample temperature. At the same time, rapid densification within seconds can occur [2–7].

Since flash sintering was first reported, researchers have extensively attempted to reveal the physical mechanisms of this remarkably fast sintering process [5]. According to recent studies, the rapid densification during flash sintering seems to be mostly caused by fast heating rates [3]. It is believed that a faster heating rate minimizes the time at lower temperatures, where surface diffusion is faster than grain boundary and volume diffusion, yielding a driving force loss by particle coarsening and neck growth [8–12]. With a fast heating rate, the green body can be heated quicker to a temperature where volume and grain boundary diffusion are dominant and, thus, high driving forces for densification are preserved. Ji et al. performed a model experiment with heating rates likewise to flash sintering, but without any electric field or current involved [3]. In these experiments, the densification without electric field was very similar to flash sintering, indicating

* Corresponding author. 701 West Stadium Ave, 47907, West Lafayette, IN, USA.
E-mail address: rheinheimer@purdue.edu (W. Rheinheimer).

https://doi.org/10.1016/j.actamat.2018.12.007
1359-6454/Published by Elsevier Ltd on behalf of Acta Materialia Inc.

that the current and field did not alter the principal densification mechanisms in zirconia. In another approach, a relatively slow flash sintering process was compared to conventional sintering with a similar heating rate and temperature for strontium titanate [13]. Densification was found to be similar in flash sintering and conventional sintering, if the heating rate and temperature are comparable.

On the other hand, it was argued that there are physical mechanisms activated by the electric field and current. For example, it was proposed that the fast densification during flash sintering of zirconia is due to the formation of Frenkel pairs [14,15]. As a result, the diffusion coefficients were argued to increase which led to the enhanced densification. It was also suggested that the high local current density in the particle contact area could cause local heating over the melting point so that liquid phase sintering occurs [16–18]. However, such a liquid phase should be visible after cooling the sample and, to the authors knowledge, only one study published evidence of such a behavior for a material with very low melting temperature and the need for high sintering temperatures (sodium potassium niobate [19]) so that grain boundary melting most likely is not a general effect of flash sintering.

Overall, it seems that Joule heating and fast heating rates are sufficient to obtain a basic understanding of the current and voltage characteristics during flash sintering [4]. However, it must be pointed out that flash sintering involves extreme heating rates, densification and cooling rates. Under these conditions, the occurrence of non-equilibrium states of the material is to be expected and the structure of flash sintered material can be very different from those obtained by conventional sintering [6,20–22]. Thus, flash sintering has the potential of processing materials with non-equilibrium features such as dislocations, non-equilibrium defect configurations, compositional gradients or metastable phases [20,23–26].

To establish an equilibrium environment to study the impact of electric fields on defects, grain growth in electric field with blocking electrodes was studied in strontium titanate [27,28]. Since densification and Joule heating did not occur in these experiments, the impact of electric field on the material can be evaluated in greater detail. Strontium titanate is a model electroceramic with vast knowledge available on defect chemistry [29], point defect formation and structure [30], grain boundary structure [30–33] and stoichiometry [31,32,34,35], space charge [34–36] and microstructure evolution [37–41]. Grain growth under an electric field revealed the occurrence of a gradient in microstructure with coarser grain size close to the negative electrode. The authors argue that this is caused by a gradient of the oxygen vacancy concentration over the entire sample implied by the electric field. In this framework, the high oxygen vacancy concentration results in a reduced material on the negative electrode as sketched in Fig. 1a. For strontium titanate, it is known that grain growth kinetics are faster in a reducing atmosphere [42]. The mechanism was explained by the change of space charge by the local oxygen vacancy concentration (Fig. 1b and c): In reduced strontium titanate, little space charge is expected based on a thermodynamic calculation [28]. In oxidized strontium titanate, a pronounced space charge is evident with strontium vacancies being accumulated at the grain boundary [34,35]. If now grain growth occurs, a diffusional drag of these accumulated defects is likely to retard grain boundary migration and, thus, slower grain growth occurs [41,43].

While gradient in microstructures were reported for many flash sintered materials [24], there are not many cases where the mechanism of this gradient was considered in detail [6]. The present study considers the interplay of electric currents and fields during flash sintering with the defect chemistry in undoped and acceptor doped strontium titanate. The focus of the work is on

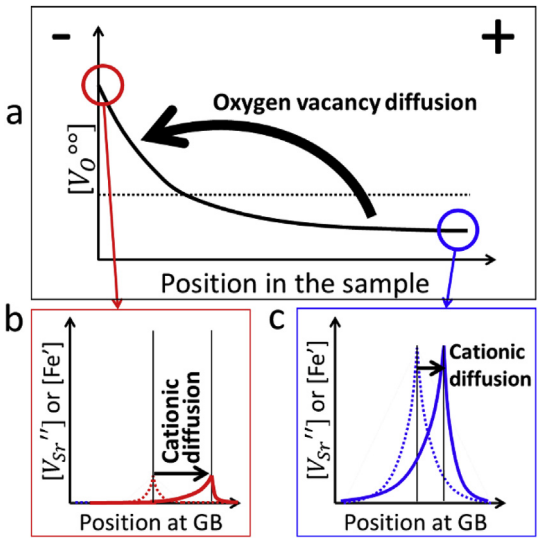

Fig. 1. Sketch of the proposed defect migration model for microstructure evolution in electric field [27,28]. A migration of the oxygen vacancies towards the negative electrode in electric field (a) results in the formation of reduced material at the negative electrode (b) and oxidized material on the positive electrode (c). For oxidizing conditions, much stronger space charge and defect segregation was reported than for reducing conditions [27,28,36,44].

gradients in the microstructure in their correlation to the electric field and the interfacial stoichiometry. Since the thermodynamics of space charge and segregation are known, the interfacial stoichiometry was considered to correlate with the local oxygen vacancy concentration. To gain insight into the impact of defect chemistry, various acceptor dopant concentrations were analyzed. The results show evidence of grain size gradients across the sample. EDS measurements showed that space charge seems to only exist on the positive electrode, which correlates well with the observations on field-assisted grain growth. Overall, the present study underlines that basic knowledge on defect chemistry and space charge still holds for flash sintering.

2. Experimental procedure

Strontium titanate powder was prepared by a mixed oxide/carbonate route based on high purity raw materials ($SrCO_3$ and TiO_2, purity of 99.95% and 99.995%, Sigma Aldrich Chemie GmbH, Taufkirchen, Germany). The A/B ratio was 0.996. Iron oxide (Fe_2O_3, purity > 99%, Merck, Darmstadt, Germany) was used as dopant. While it is known that Fe ions in the perovskite lattice may have varying valency [45,46], a valency of +3 and an occupation of the B-site of the perovskite lattice was assumed for powder processing. Charge compensation was assumed to be by oxygen vacancies and holes. The dopant concentration was 0.2, 2 and 5 at.% with respect to the B-site of the perovskite lattice. Further details of the powder synthesis are published elsewhere [37,43,47]. Cylindrical green bodies (diameter of 10 mm, length of 10 mm) were pressed uniaxially in a steel die and subsequently cold isostatically at 400 MPa. The resulting green density was 62.5 ± 1% for all green bodies.

Flash sintering experiments where performed in a rod-type dilatometer (402 E/2, Netzsch, Selb, Germany). Platinum wire spirals and cables were used to contact the sample. An uncovered thermocouple was placed close to the sample (ca. 1 mm distance) to record the sample temperature during flash sintering as accurately as possible.

The furnace was ramped up to 1200 °C at 10K/min. After reaching 1200 °C, the furnace was powered off. During the entire

experiment, a laboratory power supply (XG 600−2.8, Ametek, San Diego, USA) was used to apply a voltage to the sample. The voltage limit was set to obtain 140V/cm on the green body while the current limit was set to 250 mA. This voltage and current limit was chosen to result in slow flash sintering to obtain a sintering process that is easy to capture and analyze [13]. During the experiment, the data (shrinkage, sample temperature, voltage, current) was logged twice per second with a standard data logger (Graphtec, Irvine, USA).

For TEM observation, the samples were sectioned to prepare plan-view TEM samples close to the positive and negative electrode. Manual grinding, polishing, dimpling and final polishing in an ion milling system (PIPS II, Gatan) were conducted for TEM sample preparation and microstructure characterization was performed using an FEI TALOS 200X TEM operated at 200 kV with ChemiSTEM technology (X-FED and SuperX EDS with four silicon drift detectors) for elemental mapping.

3. Results and discussion

3.1. Flash sintering

The data of the sintering processes are shown in Fig. 2a–d. In each figure, the upper graph gives the sample temperature as measured by the thermocouple close to the sample and the relative shrinkage $\Delta L/L_0$. The lower graph contains the voltage V (right y-axis), current I (inner left y-axis) and electric power $P = U \cdot I$ (outer right y-axis).

Due to the nature of flash sintering, the sample is heated during the process by the electric power dissipated in the sample (Joule heating). Although the sample temperature was measured as close as possible to the sample, the measured temperature is an underestimation of the true sample temperature. An overheating during flash sintering of about 200K above the furnace temperature is expected as estimated by a blackbody radiation approach for strontium titanate and the same power density [13]. According to this approach, the sample temperature most likely reached 1400 °C. However, the blackbody radiation approach contains many assumptions and cannot considered to be a precise estimate of the true sample temperature.

As the field was applied before heating the furnace, at some time during the heating ramp the conductivity of the strontium titanate increases enough to allow a significant electric current flow through the sample [29]. This increase of the current starts at 1014 °C for undoped strontium titanate (Fig. 2a), at 940 °C for 0.2% Fe (Fig. 2b), at 840 °C for 2% Fe (Fig. 2c) and at 697 °C for 5% Fe (Fig. 2d). More details can be found in Table 1.

For 5% Fe, a short peak of the current and power is evident after 4280s. At the same time the sample temperature increases slightly, and some densification occurs. Accordingly, this first peak represents a flash sintering event. However, flash sintering stopped again after 200s since the sample cracked during sintering along the current direction; most likely the contact of the electrodes was changed or partly lost thereby stopping the sintering process again.

The main increase of current and shrinkage of the sample occurs shortly after the first small peak. As argued in the literature [3,4], this is because of a thermal runaway. Throughout this manuscript we refer to this as the flash sintering event. For the following quantification, we consider the flash sintering event to happen when the power source switches to current controlled output. The flash sintering event occurred at 1141 °C for undoped strontium titanate (Fig. 2a), at 1098 °C for 0.2% Fe (Fig. 2b), at 978 °C for 2% Fe (Fig. 2c) and at 854 °C for 5% Fe (Fig. 2d). The onset temperature of undoped strontium titanate corresponds well with literature data [48].

For all four flash sintering experiments, the electric power shows a maximum for this instant and subsequently decreases until the maximum temperature of the furnace is reached after 6730s. This decrease is again because of the decreasing voltage due to the increasing conductivity of strontium titanate with temperature [29]. For the same reason, the electric power and voltage increase while the furnace cools down. For undoped strontium titanate, 0.2% Fe and 2% Fe, the voltage limit is reached during cooling, so that the current is dropped by the power source. The decreasing power dissipation then drops the sample temperature, so that an inverse thermal runaway occurs (at 470 °C for undoped strontium titanate, at 597 °C for 0.2% Fe and at 504 °C for 2% Fe). For 5% Fe, an inverse thermal runaway did not occur during cooling of the furnace and the sample remained in a self-heating state until the power source was switched off.

Considering the linear shrinkage curves, densification starts to occur once the flash sintering event occurred (ignoring the peak in power and densification for 5% Fe discussed above). The abrupt length changes for undoped strontium titanate, 0.2% Fe and 2% Fe during cooling are because of thermal expansion and a fast cooling during the inverse thermal runaway. Highest densification was reached for undoped strontium titanate ($\Delta L/L_0 = -0.155$, relative density of $\rho_{rel} = 96.3\%$) followed by 0.2% Fe ($\Delta L/L_0 = -0.128$, $\rho_{rel} = 89.7\%$), 2% Fe ($\Delta L/L_0 = -0.119$, $\rho_{rel} = 87.6\%$) and 5% Fe ($\Delta L/L_0 = -0.069$, $\rho_{rel} = 76.5\%$). A similar observation where less densification occurred for higher Fe concentration was found for conventional sintering using the same powder preparation method [38]. Accordingly, the densification in the presented flash sintering experiments is similar to conventional sintering as reported before for a very similar experimental setup [13].

The characteristics of flash sintering of Fe-doped strontium titanate reflect the conductivity properties of this material. First, an increasing temperature results in higher conductivity for undoped material or for a fixed acceptor concentration [29,45,49]. This property renders flash sintering possible in strontium titanate. Second, an increasing acceptor dopant concentration results in increasing conductivity, too. This is because acceptors are compensated by oxygen vacancies and a high oxygen vacancy concentration increases the ionic conductivity [49].

The second property impacts the onset temperature of the flash sintering event. The thermal runaway in the flash sintering event requires significant current to flow through the sample to obtain a self-heating of the sample. To reach this significant current at a fixed voltage, a minimum conductivity needs to be reached by heating the sample with the furnace. If the sample conductivity is increased by doping, a lower temperature is needed for the flash sintering event. As discussed above, the data in Fig. 2 show this effect, so that the behavior of flash sintering seems to agree well with the basic defect chemistry of strontium titanate.

3.2. Microstructure

The microstructure of undoped, 2% Fe and 5% Fe-doped strontium titanate was investigated in more detail. Fig. 3 shows TEM micrographs close to the positive (a) and negative (b) electrode for the undoped strontium titanate. As expected from the relative density of 96.3%, only little remaining porosity is evident.

However, the microstructure is clearly coarser at the negative electrode compared to at the positive electrode as evident in Fig. 3. This behavior was not reported in a previous study on flash sintering of strontium titanate [13,48], possibly because it was not explicitly looked for a gradient in the grain size or because the flash sintering temperature was too low to show significant grain growth at all as argued in Ref. [13]. The selected area diffraction pattern, shown in the inset, further supports the argument that the negative

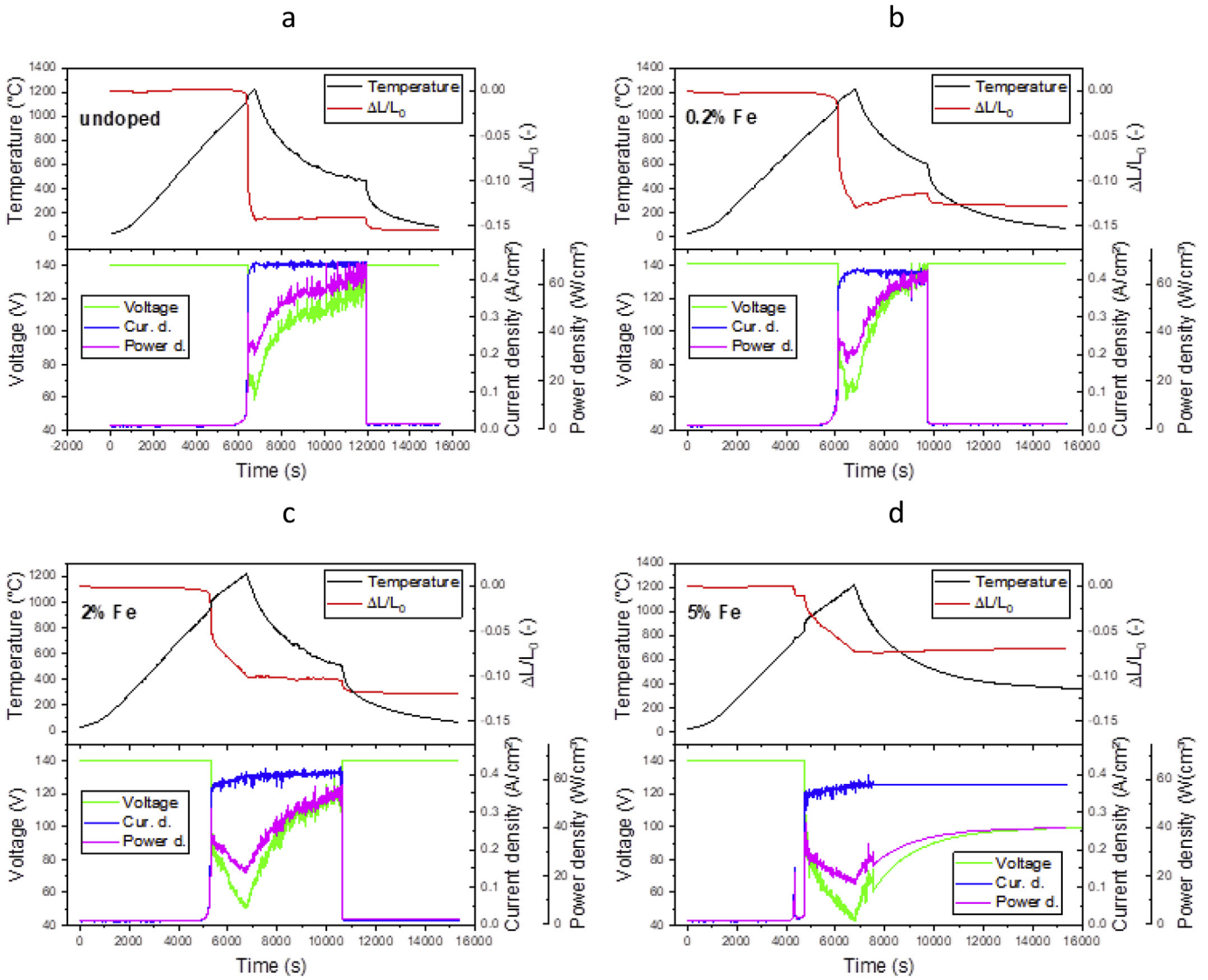

Fig. 2. Flash sintering data for undoped strontium titanate (a), for 0.2% (b), 2% (c) and 5% Fe dopant concentration (d). Each graph shows temperature and densification in the upper part and voltage, current and power dissipation in the lower part. Note that the lower graphs have 3 y axis.

Table 1
Details of the flash sintering event and final density for the four different powder compositions.

Fe dopant conc.	First significant current flow	Flash sintering onset	Final density	End of flash event during cooling
undoped	5750s or 1014 °C	6381s or 1141 °C	96.3%	11907s or 470 °C
0.2%	5370s or 940 °C	6091s or 1098 °C	89.7%	9740s or 597 °C
2%	4790s or 840 °C	5300s or 978 °C	87.6%	10613s or 504 °C
5%	4040s or 697 °C	4746s or 854 °C	76.5%	–

electrode has coarser grains. There are much fewer diffraction spots using the same aperture size, which indicates there are less grains producing a distinguished diffraction spot.

Gradients were reported for grain growth in electric field in strontium titanate in the absence of electric currents in previous studies [27,28]. In these studies, a coarser microstructure (i.e. faster grain growth) was found at the negative electrode, which agrees well with Fig. 3. Although the electric fields were estimated to be in the order of 130–270 V/cm in the cited references, it is still comparable to the field during flash sintering in the present experiments, as voltages in Fig. 2 are in the range of 50–100 V and the sample thickness is 10 mm.

The microstructures of 2% and 5% Fe-doped strontium titanate are shown in Fig. 4 as observed close to the positive (a) and negative electrodes (b). Both microstructures were found not to be fully sintered as expected from the relative density of 87.6% and 76.5%, respectively. The microstructure is much more fine-grained than for undoped strontium titanate which agrees well with the literature [38]. Similarly to undoped strontium titanate, the microstructures at the negative electrode are coarser compared to at the positive electrode, as indicated by the number of diffraction spots in the selected area diffraction pattern shown in the insets.

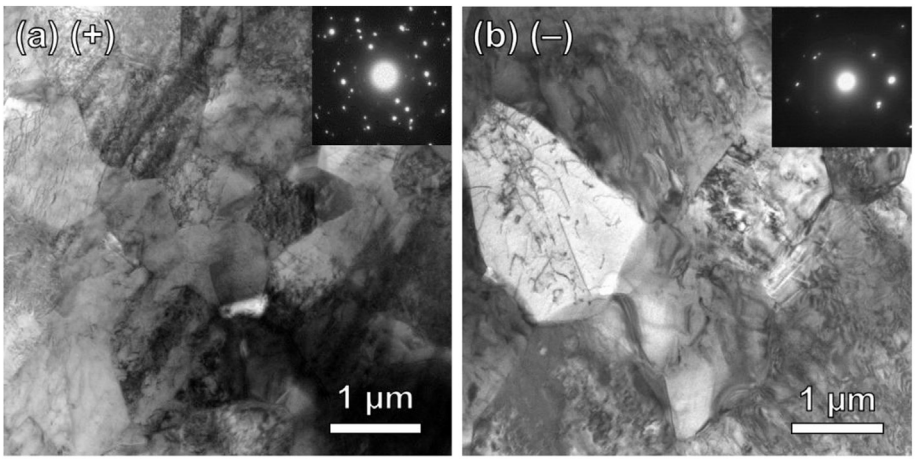

Fig. 3. Microstructures for undoped strontium titanate after flash sintering as observed by TEM close to the positive (a) and negative (b) electrode.

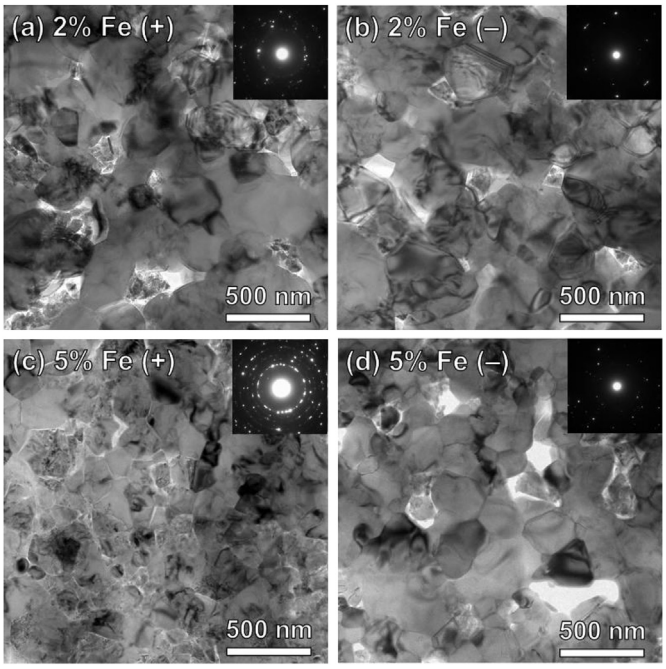

Fig. 4. Microstructures for Fe-doped strontium titanate after flash sintering as observed by TEM close to the positive (a) and negative electrode (b) for the 2% Fe and positive (c) and negative electrode(d) for the 5% Fe.

3.3. Interfacial chemistry and stoichiometry

In the literature, gradients of the grain size along the electric field were argued to be caused by a gradient in the oxygen vacancy concentration [27,28]. In this framework, it was argued that applying an electric field results in an electromigration of oxygen vacancies through the sample, resulting in a higher oxygen vacancy concentration at the negative electrode than at the positive electrode as sketched in Fig. 1a. It is known from field-free grain growth experiments that grain growth is faster in reducing atmosphere (i.e. with a high oxygen vacancy concentration) [39,41–43]. The same was found for grain growth during sintering [38]. This agrees well with the assumption of an electromigration of oxygen vacancies to the negative electrode, as faster grain growth was always found on this side.

According to a recent study, the mechanism that couples defect chemistry and grain growth is the space charge [28]. Space charge is a well-known phenomenon for perovskites [34–36,50], where the stoichiometry and point defect concentration of the grain boundary core is different from the bulk. This effect occurs because point defects (mostly vacancies) are accumulated in the boundary core to lower the grain boundary energy by an interfacial reconstruction [30,36]. As the formation energies of the respective defects ($V_{Sr}^{\circ\circ}$, and $V_{O}^{\circ\circ}$) is different, the boundary core contains different amounts of these vacancies resulting in a net charge of the grain boundary core. Analogue to standard double layer theory, a space charge layer forms in vicinity to the grain boundary to compensate the charge of the grain boundary core. Strontium titanate is known to have a positively charged grain boundary plane with a negative space charge adjacent to it [34–36]. The grain boundary core is known to be slightly Ti rich, although significant scattering was reported [31,32,34,35], while in the space charge the concentration of strontium vacancies is increased compared to the bulk [34–36]. Note that for a complete understanding of space charge and grain boundary stoichiometry the mechanical part of segregation needs to be added to this picture as lattice stress adds a driving force for segregation.

Thermodynamic modelling of space charge in strontium titanate indicates that for low $p(O_2)$ and high oxygen vacancy concentration, very little space charge (i.e. low grain boundary potential and space charge layer thickness) occurs, while for high $p(O_2)$ and low oxygen vacancy concentration a very pronounced space charge is evident (Fig. 1b and c) [28,36]. It should be noted that for strong space charge, the grain boundary is expected to be off-stoichiometric, while for less space charge the interface stoichiometry does not differ strongly from the bulk. As such, the interfacial stoichiometry is a means to probe the occurrence of space charge and to test whether the proposed electromigration of oxygen vacancies with its impact to the space charge occurs in the present flash sintering experiments as well.

Accordingly, TEM-EDS measurements were performed on undoped, 2% Fe and 5% Fe-doped strontium titanate close to the negative and positive electrode. The results for undoped strontium titanate are shown in Fig. 5. The microstructure and EDS line scan results close to the positive electrode are shown in a and c, respectively, while b and d show the same for close to the negative electrode. It is apparent that only at the positive electrode, the grain boundary core is Ti rich, while at the positive electrode no significant Ti excess is observed. These findings agree well with the discussion given above and it seems that the mechanisms found for field-assisted grain growth in strontium titanate ([27,28] and

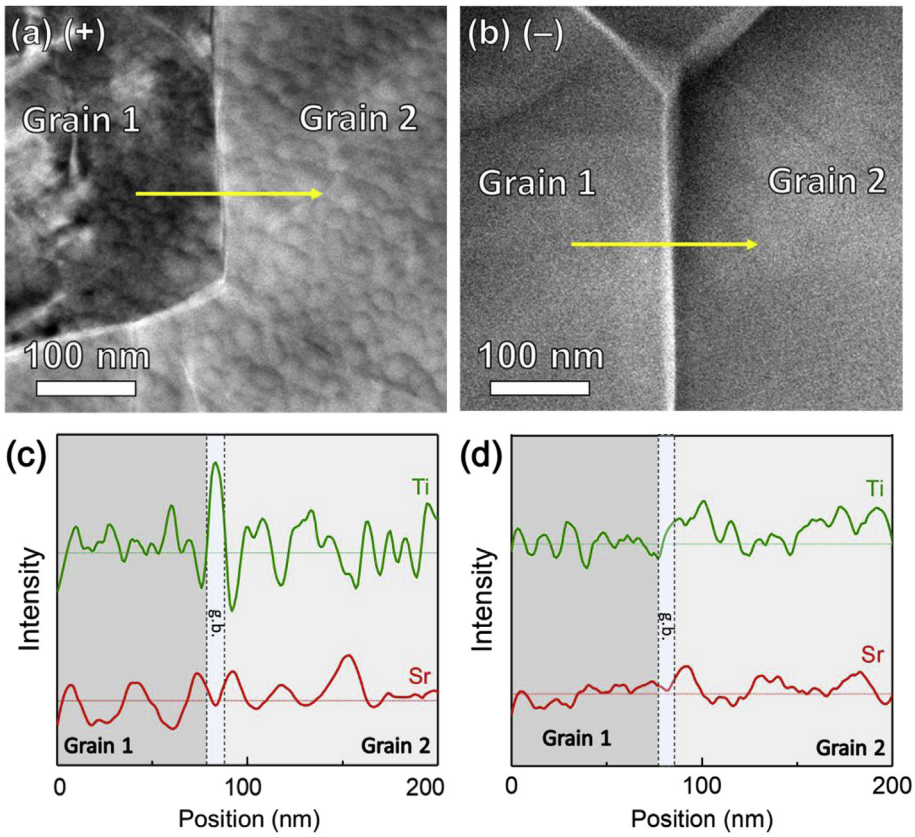

Fig. 5. STEM-HAADF of the undoped strontium titanate close to the positive (a) and negative (b) electrodes and the corresponding EDS line scan of Sr and Ti over a grain boundary (c) and (d) respectively.

Fig. 1) also apply to the present flash sintering experiments.

However, the change in stoichiometry is not very obvious as the excess of Ti at the GB core in the EDS measurements in Fig. 5 is not much higher than the noise level. To obtain more evidence, the distribution of Fe in the doped samples can be considered: if Fe is assumed to be an acceptor on the B-site of the perovskite, it is expected to accumulate in the space charge according to the negative charge of Fe'_{Ti}. As the space charge properties (i.e. grain boundary potential and its dependence on the oxygen vacancy concentration) do not change qualitatively [36], the discussion above and Fig. 1 still hold and Fe accumulation in the space charge at the boundaries is expected only where the oxygen vacancy concentration is low (i.e. at the positive electrode), while less accumulation should occur where the oxygen vacancy concentration is high (i.e. at the negative electrode).

Elemental mapping of the Fe, Sr and Ti for 2% and 5% Fe-doped strontium titanate are shown in Fig. 6. The first two rows show the data for 2% Fe at the positive (a) and negative (b) electrodes. In both cases, there is no evidence for a Ti excess at the grain boundary, but Fig. 6a shows a weak segregation of Fe at the grain boundaries at the positive electrode. No such segregation is visible at the negative electrode (Fig. 6b). The data for 5% Fe dopant concentration is shown in the last two rows for close to the positive (c) and negative (d) electrode. Again, no Ti excess is visible for both cases. However, very clear Fe segregation is visible at the positive electrode (Fig. 6c), while at the negative electrode only very little segregation occurs (Fig. 6d). As such, the findings for 2% Fe and 5% Fe dopant concentration are very similar.

EDS line scans were performed close to the positive and negative electrodes for 5% Fe-doped strontium titanate for a more quantitative comparison, as shown in Fig. 6. As expected, much stronger Fe segregation is found at the positive electrode. At the positive electrode, the measured width of the segregation layer is roughly 20 nm. At the negative electrode, the measured width is roughly 40 nm. In principle, these numbers would agree well with the expected space charge layer width for strontium titanate [28]. However, the measurement of the width of the space charge can be impacted by many experimental factors such as a tilt of the grain boundary plane with respect to the electron beam. From the present results it cannot excluded that the Fe was accumulated only in the grain boundary core and formed a very thin layer in the core. However, the solubility of Fe in strontium titanate is believed to be much higher than the present dopant concentrations, so we may assume that Fe is still situated the lattice [51–53].

Overall, these results agree well with the expectations from the discussion above and with the results for undoped strontium titanate in Fig. 5. From the presented results, we conclude that the same concepts found in the field-assisted grain growth study without current [27,28] can be applied to flash sintering: the gradients in the microstructure are very similar and the behavior of interfacial stoichiometry and space charge agree well with Fig. 1.

Certainly, the process flash sintering has a notable difference to the cited work on field-assisted grain growth [27,28]: while the grain growth experiments used blocking electrodes to prevent a current flow through the sample, these currents are a central part of flash sintering. Therefore, it needs to be discussed if, still, a gradient in the defect concentration is possible in the sample during flash sintering. It could be argued that, without blocking electrodes, the oxygen vacancies that are accumulated on the negative electrode are filled with oxygen from the atmosphere thereby leveling the

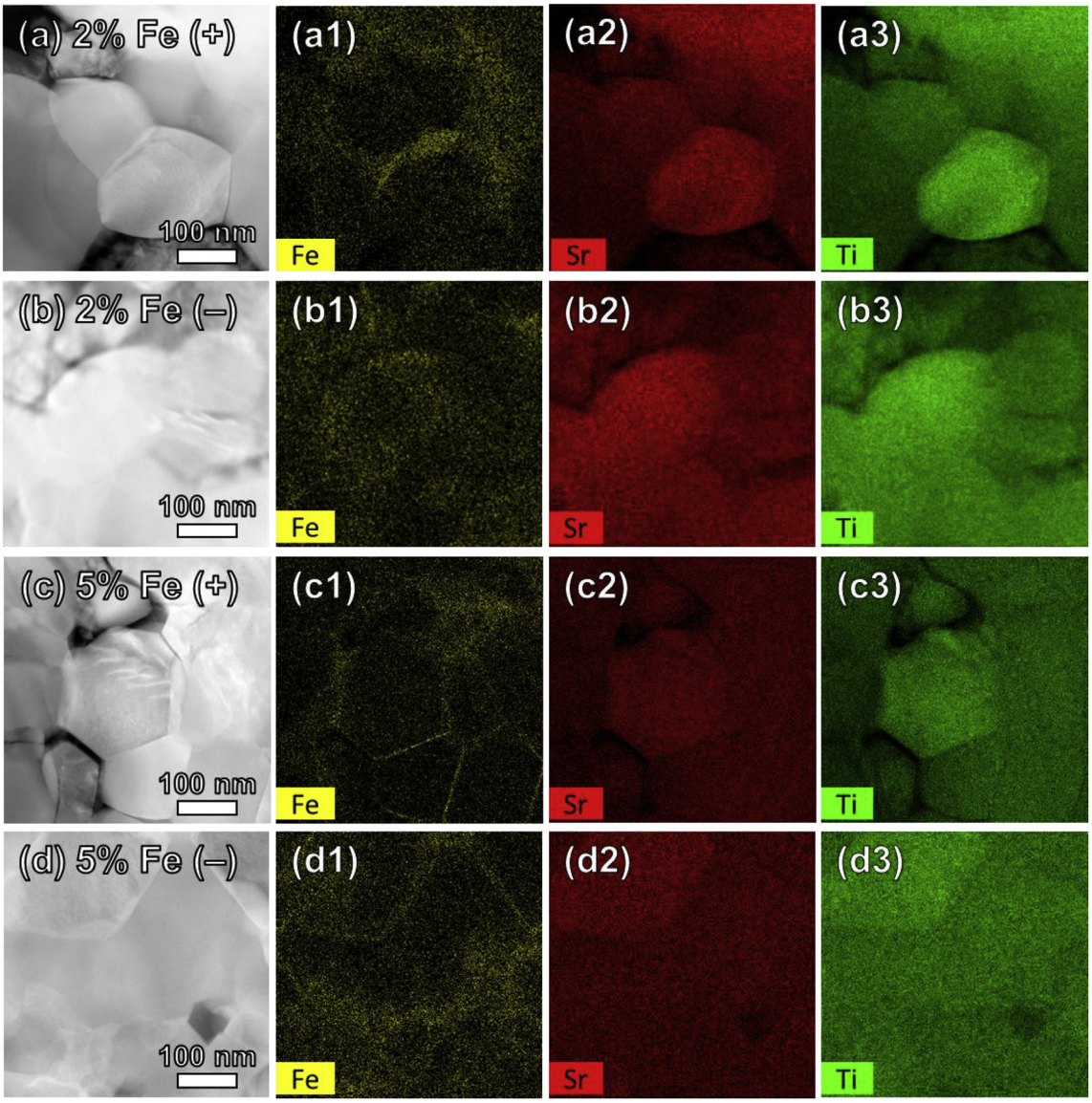

Fig. 6. Elemental mapping of Fe, Sr and Ti over a grain boundary of 2% Fe close to the positive (a) and negative (b) electrodes and 5% Fe close to the positive (c) and negative (d) electrodes. In each line, the first image shows a STEM-HAADF image, while the next three show the distribution of Fe, Sr and Ti.

gradient (see Fig. 7).

However, it must be pointed out that even during flash sintering a significant voltage drops over the sample. As Fig. 2 shows, this voltage is in the order of 60 V. Certainly, a part of this voltage drops in the platinum wires and contacts between the platinum electrode and the sample, so that the resulting field in the sample will be lower than 60 V/cm. However, the conductivity of strontium titanate is still low enough [29] so that significant field is present across the sample (an estimation yields about 40V/cm[1]). The field will result in electric currents and a separation of all mobile defects according to their polarity (positive to negative electrode and vice versa). This separation (i.e. gradient of the concentration across the sample) is expected independently of the occurrence of an electric current as long as an electric field is present across the sample.

Another uncertainty is a possible impact of cooling on both the overall defect gradient in the sample and the chemistry of the grain boundary. The experimental setup involved electric fields applied to the sample while the temperature was high. Parts of the cooling (the reverse thermal runaway) happened rapidly. The overall gradient of the oxygen vacancies after cooling might be changed since oxygen diffusion in strontium titanate is very fast. However, we do not consider the gradient directly, but only indirectly via the resulting grain boundary stoichiometry. Since a change of the grain boundary stoichiometry requires diffusion of metal ions, it can be assumed that below 800 °C a change will most likely not occur because of the low diffusion coefficients of metal ions. During cooling, this temperature was reached while an electric field was still applied so that the grain boundary stoichiometry still should

[1] The conductivity data from the literature [29] suggests a conductivity of about 10^{-2} $(\Omega cm)^{-1}$. After sintering, the samples had a diameter of about 0.9 cm and a length of about 0.9 cm. Ignoring the porosity the estimated resistance of the sample during flash sintering is 140 Ω. Given a current of 250 mA a voltage drop of about 35 V or a field of about 40 V/cm is expected, which is less than the measured 60V/cm, but still significant and in the same range as a study on field-assisted grain growth in strontium titanate where microstructural gradients were shown [27]. The remaining field most likely drops to a minor part in the platinum cables (estimated resistance of 2 × 0.5 m long cable with 0.5 mm diameter is less than 5Ω) and to a major part at the contacts.

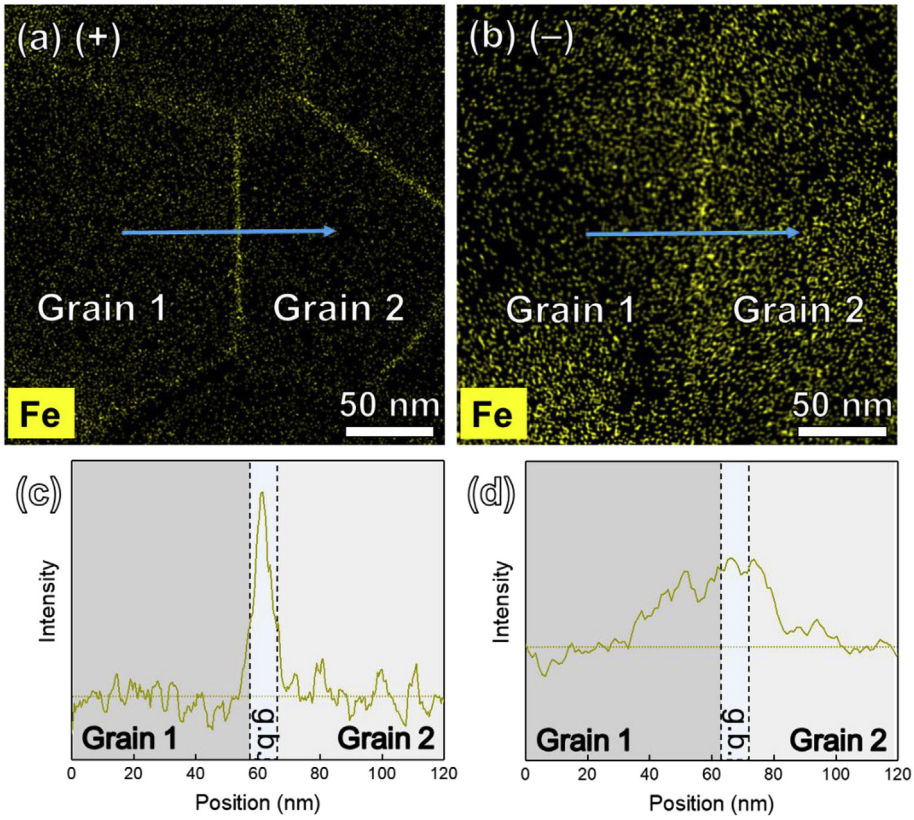

Fig. 7. Elemental mapping of Fe over a grain boundary for the 5% Fe-doped strontium titanate close to the positive (a) and negative (b) electrodes and their corresponding Fe line scan (c,d).

represent the gradient in the defect concentration.

Experimental uncertainty also arises from the valency of the Fe dopant: it is known that Fe can have different valency in strontium titanate (3 + or 4+) depending on defect chemical parameters [45,46]. As a change in the valency would change the segregation tendency of Fe at the grain boundaries, an impact of a change of the valency would impact the presented results. However, it seems not to be known how the valency changes at grain boundaries and in the electric field, so that the details of this influence seem to remain unclear.

Finally, it must be pointed out that many factors (e.g. the grain boundary misorientation [54]) impact the grain boundary stoichiometry so that the grain boundary stoichiometry of strontium titanate is known to vary in the microstructure [31,32]. Consequently, we must conclude that the presented results only represent a qualitative analysis and better statistics are needed to obtain quantitative results that would be comparable with thermodynamic calculations [28,36].

3.4. Implications for field-assisted processing in other materials

The present study reveals the occurrence of gradients of the point defect concentration caused by the electric field during flash sintering. As a consequence, microstructural gradients appear between the electrodes because microstructural evolution depends on the local point defect concentration. In the case of strontium titanate, the underlying mechanism for the coupling between local point defect chemistry and microstructure evolution seems to be the space charge at the grain boundary and its consequences on transport during microstructure evolution. However, the observed mechanism can be generalized to other materials if the following general conditions hold:

1) Existence of charged point defects with high mobility in electric fields
2) Relatively low conductivity, so that some electric field can be induced during flash sintering
3) A dependence of grain boundary properties on local point defect chemistry

Consequently, other perovskites with very similar defect chemistry and space charge properties are expected to show a similar behavior as reported here for strontium titanate. Indeed, similar microstructural gradients in electric fields were reported e.g. for barium titanate [55,56] which has almost identical defect chemistry [57] and space charge properties [34,35] as strontium titanate.

Zirconia is one of the most important model systems for flash sintering [1,5] and also well-known to show microstructural gradients after flash sintering [5,58–60]. The work by I-Wei Chen and co-authors suggests that this gradient is also caused by a gradient of point defects and possibly a valency change of the zirconium ions [60–62]. Some of these studies reported a larger grain size at the negative electrode which would agree well with the present findings for strontium titanate. However, the literature on microstructural gradients in flash-sintered zirconia is controversial as there are temperature gradients involved [63] and the details of the underlying physics of these gradients can be different than in strontium titanate as defect chemistry and segregation properties are different. However, space charge and segregation also occur in zirconia [64,65] so a similar mechanism might occur.

Titania was shown recently to form graded microstructures

during flash sintering [20]. In this case a coarser grain size was found at the positive electrode. As titania is known to have space charge at the boundaries [66,67] and the diffusion of point defects in electric fields seems to be sufficiently fast at elevated temperatures [68], it is very likely that the mechanism causing the microstructural gradients in titania is very similar to Strontium titanate.

For zinc oxide, a coarser microstructure was found at the positive electrode similar to titania after flash sintering [6]. The authors argue that a defect chemistry induced transition occurs at the interfaces yielding higher grain boundary mobility. A dependence on the oxygen partial pressure was shown [69] which seems to indicate a close relationship to the mechanism reported in this study.

Other materials like $MgAl_2O_4$ [70] also develop graded microstructures during flash sintering and the present study gives new insight into our understanding why this is the case. Also, the current findings can be extended to other materials properties than grain boundary mobility. E.g. the conductivity of ionic materials strongly depends on the local conductivity, so that a gradient in the point defect concentrations will result in a gradient of the conductivity. As such, we must consider that the electric field, power density, and temperature are not constant between the electrodes but show a gradient during flash sintering.

3.5. Implications to the grain growth transition of strontium titanate

Strontium titanate is well-known for its grain growth transition in the absence of electric fields: the grain growth coefficient decreases by orders of magnitude with increasing temperature between 1350 °C and 1425 °C [39]. In the transition range bimodal microstructures where reported [40,41]. Overall the existence and co-existence of two different grain boundary types seems to cause the counterintuitive grain growth behavior of strontium titanate [39,71]. However, the physical difference between these two types is not well-understood yet. It was suggested that this transition is related to the space charge at the grain boundaries [41]. While the presented data does not consider grain growth in detail, it does show that a correlation exists between the grain boundary chemistry and the grain growth behavior: if there is no segregation or stoichiometry change at the grain boundaries (i.e. at the negative electrode), grain growth is faster than without segregation or a different stoichiometry of the grain boundaries (i.e. at the positive electrode). Accordingly, one outcome of the present study is the importance of grain boundary chemistry and space charge for microstructural evolution.

It was suggested recently that the underlying mechanism for the dependence of grain boundary migration on space charge is diffusional drag [28]: if strong space charge and segregation of cationic point defects exists, the segregated defects diffuse along with the grain boundary yielding slow migration rates. If space charge and segregation are reduced, the migration rate is expected to be higher due to less diffusion needed to move the boundary. Applying this concept to the grain growth transition of strontium titanate one might suggest that the grain growth transition and the two grain boundary types are two different space charge states. In this case, a TEM study of the grain boundary chemistry and stoichiometry considering large and small grains separately should shed light on the physical mechanism of the grain growth transition. Preliminary investigations revealed for large grains (i.e. grains with fast migration rate) a more or less stoichiometric boundary while small grains were shown to have significant segregation and space charge [31,32]. These findings agree well with the presented results so that a correlation of space charge and grain boundary migration rate seems to be likely for the grain growth transition of strontium titanate in the absence of electric fields.

4. Summary and conclusions

This work investigates the impact of defect chemistry and field-induced point defect gradients on space charge and microstructure evolution during flash sintering of a perovskite oxide, strontium titanate. To gain more insight in the impact of point defect chemistry, different acceptor dopant levels were considered.

The onset temperature of flash sintering was shown to decrease with increasing acceptor dopant concentration as expected by the increasing conductivity for this case. The final densities were the highest for undoped strontium titanate, which agrees well with findings for conventional sintering. An increasing acceptor dopant concentration yielded a smaller grain size after flash sintering. For all compositions, a gradient of the grain size was found after flash sintering with larger grains at the negative electrode compared to at the positive electrode. TEM-EDS measurements revealed Ti-rich grain boundaries (undoped) and acceptor segregation (Fe-doped) at the positive electrode. In contrast, stoichiometric boundaries and no acceptor segregation were observed at the negative electrode, which is unexpected for strontium titanate in oxidizing atmosphere.

Based on these results, a mechanism was established that links the microstructure gradients to a field induced gradient of point defects, i.e., at the negative electrode, a higher oxygen vacancy concentration is present compared to the positive electrode. From thermodynamic modelling of space charge in strontium titanate, it is known that for higher oxygen vacancy concentration less space charge and segregation occur. This corresponds well to the experimental findings from TEM-EDS. The link between space charge and grain boundary migration rate was argued to be a diffusional drag of segregated defects yielding slow migration for strong segregation at the positive electrode and fast migration for low segregation at the negative electrode.

This mechanism could be generalized to other materials if three conditions are fulfilled: 1.) the existence of mobile charged defects, 2.) the presence of an electric field in the sample and 3.) a dependence of grain boundary properties on local point defect chemistry. It seems that these three conditions are given for many functional oxide ceramics. As many other materials are known to show microstructural gradients after flash sintering, the present relationship between defect chemistry, field-induced point defect gradients, space charge and grain boundary migration sheds new light on the basic mechanisms that are needed to understand microstructure evolution during flash sintering. Additionally, the study underlines the general importance of space charge for grain boundary migration.

Acknowledgement

A part of the work at KIT was supported by the German Research Foundation under grant no. HO 1165/20-1 within the priority programme SPP1959. X. P., Han W. and H. W. would like to acknowledge the support from the U.S. Office of Naval Research (Contract number: N00014-17-1-2087 and N00014-16-1-2778).

References

[1] M. Cologna, B. Rashkova, R. Raj, Flash sintering of nanograin zirconia in < 5 s at 850 degrees c, J. Am. Ceram. Soc. 93 (2010) 3556–3559.
[2] Y.H. Dong, I.W. Chen, Thermal runaway in mold-assisted flash sintering, J. Am. Ceram. Soc. 99 (2016) 2889–2894.
[3] W. Ji, B. Parker, S. Falco, J.Y. Zhang, Z.Y. Fu, R.I. Todd, Ultra-fast firing: effect of heating rate on sintering of 3ysz, with and without an electric field, J. Eur. Ceram. Soc. 37 (2017) 2547–2551.
[4] R.I. Todd, E. Zapata-Solvas, R.S. Bonilla, T. Sneddon, P.R. Wilshaw, Electrical characteristics of flash sintering: thermal runaway of joule heating, J. Eur. Ceram. Soc. 35 (2015) 1865–1877.

[5] M. Yu, S. Grasso, R. Mckinnon, T. Saunders, M.J. Reece, Review of flash sintering: materials, mechanisms and modelling, Adv. Appl. Ceramics 116 (2017) 24–60.
[6] Y.Y. Zhang, J.I. Jung, J. Luo, Thermal runaway, flash sintering and asymmetrical microstructural development of zno and zno-bi2o3 under direct currents, Acta Mater. 94 (2015) 87–100.
[7] Y.Y. Zhang, J.Y. Nie, J.M. Chan, J. Luo, Probing the densification mechanisms during flash sintering of zno, Acta Mater. 125 (2017) 465–475.
[8] D.E. Garcia, J. Seidel, R. Janssen, N. Claussen, Fast firing of alumina, J. Eur. Ceram. Soc. 15 (1995) 935–938.
[9] M. Harmer, R. Brook, Fast firing: microstructural benefits, J. Br. Ceram. Soc. 80 (1981) 147–148.
[10] D.L. Johnson, Ultra-rapid sintering of ceramics, in: D.P. Uskokovi, H. Palmour, R.M. Spriggs (Eds.), Science of Sintering, Springer, Boston, MA, 1989, pp. 497–506.
[11] A.N. Klein, D. Hotza, Advanced ceramics with dense and fine-grained microstructures through fast firing, Rev. Adv. Mater. Sci. 30 (2012) 273–281.
[12] P. Vergnon, F. Juillet, S. Teichner, Effect of increasing rate of temperature on sintering of pure alumina homodispered particles, Rev. Int. Hautes Temp. Refract. 3 (1966) 409–419.
[13] F. Lemke, W. Rheinheimer, M.J. Hoffmann, A comparison of power controlled flash sintering and conventional sintering of strontium titanate, Scripta Mater. 130 (2017) 187–190.
[14] R. Raj, M. Cologna, J.S.C. Francis, Influence of externally imposed and internally generated electrical fields on grain growth, diffusional creep, sintering and related phenomena in ceramics, J. Am. Ceram. Soc. 94 (2011) 1941–1965.
[15] K. Terauds, J.M. Lebrun, H.H. Lee, T.Y. Jeon, S.H. Lee, J.H. Je, R. Raj, Electroluminescence and the measurement of temperature during stage iii of flash sintering experiments, J. Eur. Ceram. Soc. 35 (2015) 3195–3199.
[16] R. Chaim, Liquid film capillary mechanism for densification of ceramic powders during flash sintering, Materials 9 (2016) 280.
[17] J. Narayan, Grain growth model for electric field-assisted processing and flash sintering of materials, Scripta Mater. 68 (2013) 785–788.
[18] J. Narayan, A new mechanism for field-assisted processing and flash sintering of materials, Scripta Mater. 69 (2013) 107–111.
[19] G. Corapcioglu, M.A. Gülgün, K. Kisslinger, S. Sturm, S. Jha, R. Raj, Microstructure and microchemistry of flash sintered k0.5na0.5nbo3, J. Ceram. Soc. Jpn. 124 (2016) 321–328.
[20] H. Charalambous, S.K. Jha, H. Wang, X.L. Phuah, H. Wang, T. Tsakalakos, Inhomogeneous reduction and its relation to grain growth of titania during flash sintering, Scripta Mater. 155 (2018) 37–40.
[21] J.M. Lebrun, T.G. Morrissey, J.S.C. Francis, K.C. Seymour, W.M. Kriven, R. Raj, Emergence and extinction of a new phase during on-off experiments related to flash sintering of 3ysz, J. Am. Ceram. Soc. 98 (2015) 1493–1497.
[22] B. Yoon, D. Yadav, R. Raj, E.P. Sortino, S. Ghose, P. Sarin, D. Shoemaker, Measurement of o and ti atom displacements in tio2 during flash sintering experiments, J. Am. Ceram. Soc. 101 (2018) 1811–1817.
[23] J. Cho, Q. Li, H. Wang, Z. Fan, J. Li, S. Xue, K.S.N. Vikrant, H. Wang, T.B. Holland, A.K. Mukherjee, R.E. Garcia, X. Zhang, High temperature deformability of ductile flash-sintered ceramics via in-situ compression, Nat. Commun. 9 (2018) 2063.
[24] J. Luo, The scientific questions and technological opportunities of flash sintering: from a case study of zno to other ceramics, Scripta Mater. 146 (2018) 260–266.
[25] X.L. Phuah, H. Wang, H. Charalambous, S.K. Jha, T. Tsakalakos, X. Zhang, H. Wang, Comparison of the grain growth behavior and defect structures of flash sintered ZnO with and without controlled current ramp, Scripta Mater. 162 (2019) 251–255.
[26] H. Wang, X. Phuah, J. Li, T.B. Holland, R.E. Garcia, A. Mukherjee, X. Zhang, H. Wang, Key microstructural characteristics in flash sintered 3ysz critical for enhanced sintering process, Ceram. Int. 45 (2019) 1251–1257.
[27] W. Rheinheimer, M. Fülling, M.J. Hoffmann, Grain growth in weak electric fields in strontium titanate: grain growth acceleration by defect redistribution, J. Eur. Ceram. Soc. 36 (2016) 2773–2780.
[28] W. Rheinheimer, J.P. Parras, J.-H. Preusker, R.A.D. Souza, M.J. Hoffmann, Grain growth in strontium titanate in electric fields: the impact of space charge on the grain boundary mobility, J. Am. Ceram. Soc. (2018), https://doi.org/10.1111/jace.16217.
[29] R. Moos, K. Härdtl, Defect chemistry of donor-doped and undoped strontium titanate ceramics between 1000°c and 1400°c, J. Am. Ceram. Soc. 80 (1997) 2549–2562.
[30] S. von Alfthan, N.A. Benedek, L. Chen, A. Chua, D. Cockayne, K.J. Dudeck, C. Elsaesser, M.W. Finnis, C.T. Koch, B. Rahmati, M. Rühle, S.-J. Shih, A.P. Sutton, The structure of grain boundaries in strontium titanate: theory, simulation, and electron microscopy, in: D. Clarke, M. Ruhle, F. Zok (Eds.), Annual Review of Materials Research, 2010, pp. 557–599, 40 of Annual Review of Materials Research.
[31] M. Bäurer, S.-J. Shih, C. Bishop, M.P. Harmer, D. Cockayne, M.J. Hoffmann, Abnormal grain growth in undoped strontium and barium titanate, Acta Mater. 58 (2010) 290–300.
[32] S.-J. Shih, S. Lozano-Perez, D.J.H. Cockayne, Investigation of grain boundaries for abnormal grain growth in polycrystalline srtio3, J. Mater. Res. 25 (2010) 260–265.
[33] H. Sternlicht, W. Rheinheimer, M.J. Hoffmann, W.D. Kaplan, The mechanism of grain boundary motion in srtio3, J. Mater. Sci. 51 (2015) 467–475.
[34] Y.-M. Chiang, T. Takagi, Grain-boundary chemistry of barium titanate and strontium titanate: I, high-temperature equilibrium space charge, J. Am. Ceram. Soc. 73 (1990) 3278–3285.
[35] Y.-M. Chiang, T. Takagi, Grain-boundary chemistry of barium titanate and strontium titanate: Ii, origin of electrical barriers in positive-temperature-coefficient thermistors, J. Am. Ceram. Soc. 73 (1990) 3286–3291.
[36] R.A. De Souza, The formation of equilibrium space-charge zones at grain boundaries in the perovskite oxide srtio3, Phys. Chem. Chem. Phys. 11 (2009) 9939–9969.
[37] M. Bäurer, H. Kungl, M.J. Hoffmann, Influence of sr/ti stoichiometry on the densification behavior of strontium titanate, J. Am. Ceram. Soc. 92 (2009) 601–606.
[38] F. Lemke, W. Rheinheimer, M. Hoffmann, Sintering and grain growth in srtio3: impact of defects on kinetics, J. Ceram. Soc. Jpn. 124 (2016) 346–353.
[39] W. Rheinheimer, M.J. Hoffmann, Non-arrhenius behavior of grain growth in strontium titanate: new evidence for a structural transition of grain boundaries, Scripta Mater. 101 (2015) 68–71.
[40] W. Rheinheimer, M. Hoffmann, Grain growth transitions of perovskite ceramics and their relationship to abnormal grain growth and bimodal microstructures, Journal of Materials Science HTC (2015) 1–10.
[41] W. Rheinheimer, M.J. Hoffmann, Grain growth in perovskites: what is the impact of boundary transitions? Curr. Opin. Solid State Mater. Sci. 20 (2016) 286–298.
[42] W. Rheinheimer, M. Bäurer, M. Hoffmann, A reversible wetting transition in strontium titanate and its influence on grain growth and the grain boundary mobility, Acta Mater. 101 (2015) 80–89.
[43] W. Rheinheimer, M. Bäurer, C. Handwerker, J. Blendell, M. Hoffmann, Growth of single crystalline seeds into polycrystalline strontium titanate: anisotropy of the mobility, intrinsic drag effects and kinetic shape of grain boundaries, Acta Mater. 95 (2015) 111–123.
[44] R.A. De Souza, Z.A. Munir, S. Kim, M. Martin, Defect chemistry of grain boundaries in proton-conducting solid oxides, Solid State Ionics 196 (2011) 1–8.
[45] J.J. Wang, H.B. Huang, T.J.M. Bayer, A. Moballegh, Y. Cao, A. Klein, E.C. Dickey, D.L. Irving, C.A. Randall, L.Q. Chen, Defect chemistry and resistance degradation in fe-doped srtio3 single crystal, Acta Mater. 108 (2016) 229–240.
[46] R. Waser, T. Baiatu, K.-H. Härdtl, Dc electrical degradation of perovskite-type titanates: Ii, single crystals, J. Am. Ceram. Soc. 73 (1990) 1654–1662.
[47] W. Rheinheimer, M. Bäurer, H. Chien, G.S. Rohrer, C.A. Handwerker, J.E. Blendell, M.J. Hoffmann, The equilibrium crystal shape of strontium titanate and its relationship to the grain boundary plane distribution, Acta Mater. 82 (2015) 32–40.
[48] A. Karakuscu, M. Cologna, D. Yarotski, J. Won, J.S.C. Francis, R. Raj, B.P. Uberuaga, Defect structure of flash-sintered strontium titanate, J. Am. Ceram. Soc. 95 (2012) 2531–2536.
[49] R.A. De Souza, Oxygen diffusion in srtio3 and related perovskite oxides, Adv. Funct. Mater. 25 (2015) 6326–6342.
[50] F. Gunkel, R. Waser, A.H.H. Ramadan, R.A. De Souza, S. Hoffmann-Eifert, R. Dittmann, Space charges and defect concentration profiles at complex oxide interfaces, Phys. Rev. B 93 (2016) 245431.
[51] M.D. Drahus, P. Jakes, E. Erdem, R.A. Eichel, Defect structure of the mixed ionic-electronic conducting sr[ti,fe]o-x solid-solution system - change in iron oxidation states and defect complexation, Solid State Ionics 184 (2011) 47–51.
[52] S. Molin, W. Lewandowska-Iwaniak, B. Kusz, M. Gazda, P. Jasinski, Structural and electrical properties of sr(ti, fe)o3-delta materials for sofc cathodes, J. Electroceram. 28 (2012) 80–87.
[53] S. Steinsvik, Y. Larring, T. Norby, Hydrogen ion conduction in iron-substituted strontium titanate, srt1-xfexo3-x/2 (0 <= x <= 0.8), Solid State Ionics 143 (2001) 103–116.
[54] A.H.H. Ramadan, R.A. De Souza, Atomistic simulations of symmetrical low-angle [100] (01l) tilt boundaries in srtio3, Acta Mater. 118 (2016) 286–295.
[55] H.R. Jin, S.H. Yoon, J.H. Lee, N.M. Hwang, D.Y. Kim, J.H. Han, Effect of external electric field on the grain growth of barium titanate in n-2 atmosphere, J. Mater. Sci. Mater. Electron. 16 (2005) 749–752.
[56] H.R. Jin, S.H. Yoon, J.H. Lee, J.H. Lee, N.M. Hwang, D.Y. Kim, J.H. Han, Effect of external electric field on the grain-growth behavior of barium titanate, J. Am. Ceram. Soc. 87 (2004) 1747–1752.
[57] D.M. Smyth, The Defect Chemistry of Metal Oxides (Monographs on the Physics and Chemistry of Materials), Oxford University Press, 2000.
[58] S. Ghosh, A.H. Chokshi, P. Lee, R. Raj, A huge effect of weak dc electrical fields on grain growth in zirconia, J. Am. Ceram. Soc. 92 (2009) 1856–1859.
[59] S.-W. Kim, S.-J.L. Kang, I.-W. Chen, Electro-sintering of yttria-stabilized cubic zirconia, J. Am. Ceram. Soc. 96 (2013) 1398–1406.
[60] S.-W. Kim, S.G. Kim, J.-I. Jung, S.-J.L. Kang, I.-W. Chen, Enhanced grain boundary mobility in yttria-stabilized cubic zirconia under an electric current, J. Am. Ceram. Soc. 94 (2011) 4231–4238.
[61] Y.H. Dong, I.W. Chen, Electrical and hydrogen reduction enhances kinetics in doped zirconia and ceria: Ii. mapping electrode polarization and vacancy condensation in ysz, J. Am. Ceram. Soc. 101 (2018) 1058–1073.
[62] Y.H. Dong, H.R. Wang, I.W. Chen, Electrical and hydrogen reduction enhances kinetics in doped zirconia and ceria: I. grain growth study, J. Am. Ceram. Soc. 100 (2017) 876–886.
[63] W. Qin, J. Yun, A.M. Thron, K. van Benthem, Temperature gradient and microstructure evolution in ac flash sintering of 3 mol% yttria-stabilized

zirconia, Mater. Manuf. Process. 32 (2017) 549–556.
[64] B. Feng, N.R. Lugg, A. Kumamoto, Y. Ikuhara, N. Shibata, Direct observation of oxygen vacancy distribution across yttria-stabilized zirconia grain boundaries, ACS Nano 11 (2017) 11376–11382.
[65] K. Matsui, H. Yoshida, Y. Ikuhara, Review: microstructure-development mechanism during sintering in polycrystalline zirconia, Int. Mater. Rev. 63 (2018) 375–406.
[66] J.A.S. Ikeda, Y.M. Chiang, Space-charge segregation at grain-boundaries in titanium-dioxide .1. relationship between lattice defect chemistry and space-charge potential, J. Am. Ceram. Soc. 76 (1993) 2437–2446.
[67] J.A.S. Ikeda, Y.M. Chiang, A.J. Garrattreed, J.B. Vandersande, Space-charge segregation at grain-boundaries in titanium-dioxide .2. model experiments, J. Am. Ceram. Soc. 76 (1993) 2447–2459.
[68] A. Moballegh, E.C. Dickey, Electric-field-induced point defect redistribution in single-crystal tio2-x and effects on electrical transport, Acta Mater. 86 (2015) 352–360.
[69] Y.Y. Zhang, J. Luo, Promoting the flash sintering of zno in reduced atmospheres to achieve nearly full densities at furnace temperatures of < 120 degrees c, Scripta Mater. 106 (2015) 26–29.
[70] H. Yoshida, P. Biswas, R. Johnson, M.K. Mohan, Flash-sintering of magnesium aluminate spinel (mgal2o4) ceramics, J. Am. Ceram. Soc. 100 (2016) 554–562.
[71] M.N. Kelly, W. Rheinheimer, M.J. Hoffmann, G.S. Rohrer, Anti-thermal grain growth in srtio3: coupled reduction of the grain boundary energy and grain growth rate constant, Acta Mater. 149 (2018) 11–18.